Nanoscale

PAPER

View Article Online
View Journal | View Issue

3-Dimensional photonic crystal surface enhanced upconversion emission for improved near-infrared photoresponse†

Cite this: *Nanoscale*, 2014, **6**, 817

Wenbin Niu,[a] Liap Tat Su,[a] Rui Chen,[b] Hu Chen,[a] Yi Wang,[c] Alagappan Palaniappan,[c] Handong Sun[b] and Alfred Iing Yoong Tok*[a]

The enhancement of upconversion luminescence of lanthanide-ion doped fluoride upconversion nanoparticles (UCNPs) is particularly important and highly required for their myriad applications in sensing, photoelectronic devices and bio-imaging. In this work, the amplification of luminescence in $NaYF_4$:Yb/Er and $NaYF_4$:Yb/Tm UCNPs in close proximity to the three-dimensional photonic crystal (3D PC) surface for improved near-infrared photoresponse of a carbon nanotube-based phototransistor is reported. The self-assembled opal 3D PCs with polystyrene sphere sizes of 200, 290 and 360 nm that exhibit reflection peaks of 450, 650 and 800 nm respectively were used for upconversion enhancement, and around 30 times enhancement was obtained for $NaYF_4$:Yb/Er and $NaYF_4$:Yb/Tm UCNPs. Time-resolved upconversion emission and 3D PC transmittance-dependent upconversion enhancement reveal that the enhanced absorption and the extraction effects, resulting from the enhanced non-resonant pump excitation field and the strong coherent scattering provided by 3D PCs respectively, are responsible for the large enhancement. As a proof-of-concept experiment, the prepared 3D PC/$NaYF_4$:Yb/Tm UCNP coupled material layer was introduced into the carbon nanotube-based phototransistor. It is shown that the photoresponsivity of the device to near-infrared light was improved by 10 times with respect to the control device with carbon nanotubes only, which reveals the promising applications of this coupled material in photoelectronic devices such as photovoltaics and other types of phototransistors.

Received 12th September 2013
Accepted 26th October 2013

DOI: 10.1039/c3nr04884e

www.rsc.org/nanoscale

Introduction

Upconversion materials are materials which can convert two or more sub-bandgap photons into one above-bandgap photon. Due to their photon upconversion, they have recently attracted great attention with wide applications in solar cells,[1] 3-dimensional displays,[2] sensing,[3–5] biological labeling and imaging.[4,6,7] Among the current upconversion materials, Yb/Er and Yb/Tm co-doped hexagonal phase $NaYF_4$ has been shown to be the most effective upconverter,[8] because of the low phonon energy of the $NaYF_4$ host which can suppress the non-radiative multiphonon relaxation processes of the lanthanide dopants. However, upconversion nanoparticles (UCNPs) are still suffering from the low emission efficiency (*e.g.* 0.1% for the $NaYF_4$:Yb^{3+}/Er^{3+} UCNPs with the size of 30 nm),[3,7–9] due to the small absorption and emission cross-sections which arise from the formally forbidden 4f–4f transitions of the lanthanide ions.[10,11] Therefore, it is still a challenge to effectively improve the efficiency of UCNPs to realize various applications.

As such, much effort has been devoted to increase the emission efficiency of fluoride UCNPs, especially with the use of external field enhancement methods. One notable method is the coupling of metal nanostructures such as Au and Ag nanoparticles to the UCNPs.[12–15] Surfaces of metal nanostructures have a local surface-bound electric field which can increase the excitation rates and radiative decay rates of the UCNPs, and therefore improve the overall emission intensities of UCNPs.[11] Schietinger *et al.* have demonstrated gold plasmonic-enhanced upconversion emissions in single $NaYF_4$:Yb/Er nanoparticles and achieved emission enhancement factors of 4.8 by enhanced surface-bound electric fields.[12] A similar

[a]*School of Materials Science and Engineering, Nanyang Technological University, 50 Nanyang Avenue, 639798, Singapore. E-mail: MIYTok@ntu.edu.sg; Tel: +65 6790 493*
[b]*School of Physical and Mathematical Sciences, Nanyang Technological University, 50 Nanyang Avenue, 639798, Singapore*
[c]*Center of Biomimetic Sensor Science, Nanyang Technological University, 50 Nanyang Avenue, 639798, Singapore*

† Electronic supplementary information (ESI) available: XRD patterns of $NaYF_4$:Yb/Er UCNPs (Fig. S1), upconversion luminescence rise and decay curves of $NaYF_4$:Yb/Er and $NaYF_4$:Yb/Tm UCNPs (Fig. S2), angle-dependent reflectance spectra of opal PCs prepared with 200, 290 and 360 nm polystyrene spheres (Fig. S3), reflectance spectra of opal 3D PCs prepared with various concentrations of 290 nm polystyrene spheres (Fig. S4), transmittance-dependent 410 nm emission of $NaYF_4$:Yb/Er UCNPs (Fig. S5) and transmittance spectra of 3D PCs prepared with different polystyrene sphere sizes at 0.4 wt% concentration (Fig. S6). See DOI: 10.1039/c3nr04884e

enhancement based on Au and Ag plasmonic effects has also been reported by other researchers.[13,16] However, there are two inherent limitations for these plasmonic-based approaches. First, emission quenching has been shown to occur within a small distance of less than 10 nm from the surfaces of metal particles. As a result, a thin dielectric spacer layer is needed to maximize the enhancement (*e.g.* around 10 nm for Ag nanoparticles).[11,13] In addition, the large spectral width of metal's surface plasmonic resonances (~100 nm) limits the field enhancement due to the relatively low quality factor (Q, $Q = \lambda/\Delta\lambda$, λ is the wavelength of reflection or absorption peaks, $\Delta\lambda$ is the full width of half maximum) and low stored electric field intensity because of quick dissipation of energy in the metal nanoparticles.[17,18]

To overcome the limitations, photonic crystals (PCs) are sought as a solution.[19–21] Three-dimensional photonic crystals (3D PCs) are materials with periodic dielectric structures that can manipulate the flow of light and give rise to photonic bandgaps. While exhibiting the high quality factor, they have been demonstrated to have high stored electric field intensity on their surfaces.[19–21] For PCs, a highly efficient reflection represents a resonance at a specific wavelength under broadband illumination. When the PC surface is illuminated with light of the corresponding resonant wavelength, the surface-bound electric field is strongly enhanced by the resonant reflection. This, in turn, can enhance the absorption of the nanomaterials on the surface of PCs, resulting in enhanced emission without quenching effects.[22] Even at excitation wavelengths off-resonance with the PC surface, near-field optical investigations have also revealed the presence of the enhanced electric field intensity on the PC surface.[21,23] In addition, the coherent scattering phenomenon of PCs could improve the extraction of fluorescence from the PC surfaces.[24,25] It is usually combined with the enhanced absorption contributing to PC surface-enhanced fluorescence.

Here, we report the photon upconversion enhancement of fluoride UCNPs on the surface of 3D PCs and the improved photoresponsivity of single-walled carbon-nanotube (CNT) based phototransistors to near-infrared light (Scheme 1). The upconversion luminescence enhancement of more than 30 times was obtained for $NaYF_4$:Yb/Er and $NaYF_4$:Yb/Tm UCNPs. By fabricating the CNT-based near-infrared phototransistor on the surface of the $NaYF_4$:Yb/Tm UCNP coupled opal 3D PC, we successfully demonstrated the enhanced photoresponsivity to near-infrared light due to the opal surface-enhanced photon upconversion, which indicates its potential applications in photoelectric devices with enhanced near-infrared light photoresponse.

Results and discussion

$NaYF_4$:Yb/Er and $NaYF_4$:Yb/Tm UCNPs were prepared using a thermolysis method.[26,27] Fig. 1 shows transmission electron microscopy (TEM) images of the $NaYF_4$:Yb/Er and $NaYF_4$:Yb/Tm UCNPs, showing monodispersed particles of 40 nm diameter. The nanoparticles are in pure hexagonal phase (JSPDS 28-1192, Fig. S1, ESI†) and their upconversion emission spectra clearly exhibit the characteristic emission bands of the Er^{3+} ion at 550 and 655 nm and the Tm^{3+} ion at 350 and 460 nm for $NaYF_4$:Yb/Er and $NaYF_4$:Yb/Tm UCNPs.

Prior to coupling $NaYF_4$:Yb/Er and $NaYF_4$:Yb/Tm UCNPs on the surface of three-dimensional opal PCs, the opal was prepared by a vertical deposition self-assembly method.[28] The top-view images in Fig. 2a–d clearly demonstrate that opal PCs of 200, 290 and 360 nm photonic lattice sizes are in the dense face-centered cubic (fcc) arrangement with the close packed plane (111) oriented parallel to the underlying glass substrate.[28] Fig. 2e shows the typical cross-section view image of an opal PC with 290 nm polystyrene spheres and with total thickness of the opal is around 18 μm. The specular reflectance measurement shows that the opal PCs are sharp and symmetrical and the intensities are high which indicate the hierarchically ordered periodicity of the opal assembly, which is an important attribute to the high quality factor for surface resonances (Fig. 2f).

In contrast to approaches involving surface plasma on metal surfaces such as silver and gold nanoparticles, PCs could maximally enhance the emission of fluorophores that are closest to their surface without quenching.[17,18,22] To obtain the maximum upconversion enhancement of the coupled material, as-prepared UCNPs were dispersed in hexane solution and spin-coated onto the surface of opal PCs. Fig. 3 shows that a layer of nanoparticles is densely packed on the surface of the opal. The corresponding upconversion emission spectra of the $NaYF_4$:Yb/Er nanoparticles on the opal of different polystyrene sphere size of 200, 290 and 360 nm have clearly revealed the strong enhancement of emission (Fig. 4) For Er^{3+} ion emission in $NaYF_4$ nanoparticles, its characteristic emission bands centered at 540 nm and 660 nm, due to the electronic transitions of $^2H_{11/2}/^4S_{3/2} \rightarrow {}^4I_{15/2}$ and $^4F_{9/2} \rightarrow {}^4I_{15/2}$ (Fig. 4a),[29] are about 30 times stronger when coupled on the opal surface (Fig. 4c). A similar strength of enhancement is also found in $NaYF_4$:Yb/Tm nanoparticles on the surface of the opal, whose emission is ascribed to the electronic transitions $^1D_2 \rightarrow {}^3H_6$ and $^1G_4 \rightarrow {}^3H_6$ of the Tm^{3+} ion (Fig. 4b and d).[26,30] The variation of polystyrene sphere sizes in 3D PCs has no significant effect on the upconversion enhancement. In most cases, upconversion emission enhancement occurs because of the change of absorption of the excitation pump at 980 nm and emission of UCNPs. The absorption enhancement arises from the increase of the pump excitation field that increases the excitation rate of the doped lanthanide ion. The emission enhancement of UCNPs is caused by the increase of radiative rate due to the Purcell effect. Therefore, to probe the underlying mechanism of the enhanced emission of nanoparticles on the opals, their rise-time and decay rates were measured through the use of time-resolved upconversion emission.

The process of rise time for UCNPs is complicated because it involves the first and second excited level of the Er^{3+} ion, and it is related to the energy transfer rate between Yb^{3+} and Er^{3+}ions.[12,15] As a result, the rise time measurement was modified by determining the time signal rising to half of its maximal emission intensity. The time-resolved upconversion emissions of $NaYF_4$:Yb/Er and $NaYF_4$:Yb/Tm UCNPs in combination with 3D PCs with different polystyrene sphere

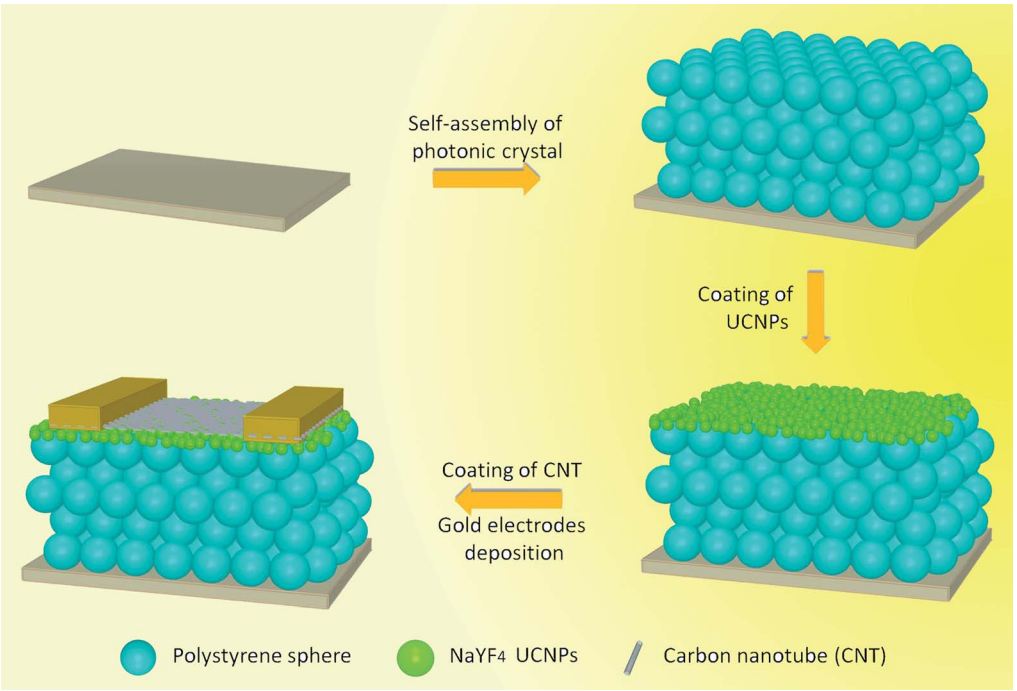

Scheme 1 A schematic representation showing the fabrication process of an enhanced near-infrared light phototransistor.

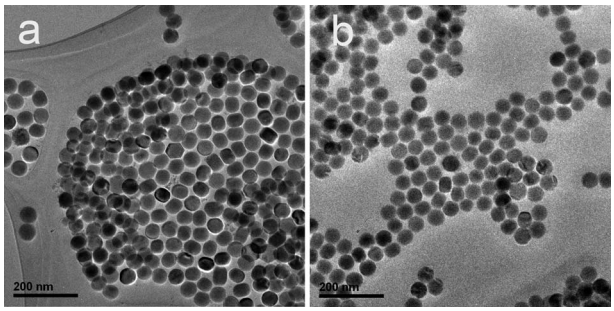

Fig. 1 TEM images of $NaYF_4$:Yb/Er (a) and $NaYF_4$:Yb/Tm (b) UCNPs.

sizes are shown in Fig. S2a and b (ESI†) respectively. Measurements revealed that the rise time for the Er^{3+} ion characteristic emission peak of 540 nm decreases from 258 μs for upconversion to 247 μs for upconversion coupled on the opal of 290 nm polystyrene spheres. Measurement of the Tm^{3+} ion characteristic emission peak of 477 nm revealed that the rise time decreases by about 4%, from 339 μs to 327 μs when the nanoparticles are coupled on the opal. As the excitation wavelength (980 nm) of UCNPs does not match with the resonant wavelengths of those opals in the present work (Fig. 2f and S3, ESI†), the rise time is only enhanced marginally due to the formation of relatively weak surface electric field intensity.[19,21,24] Nevertheless, the results indicate that the non-resonant enhancement of pump excitation field can partially contribute to the absorption enhancement of UCNPs. In addition, unlike metal-plasmon induced upconversion enhancement, there is no significant change in decay times, implying the absence of opal PC surface enhanced

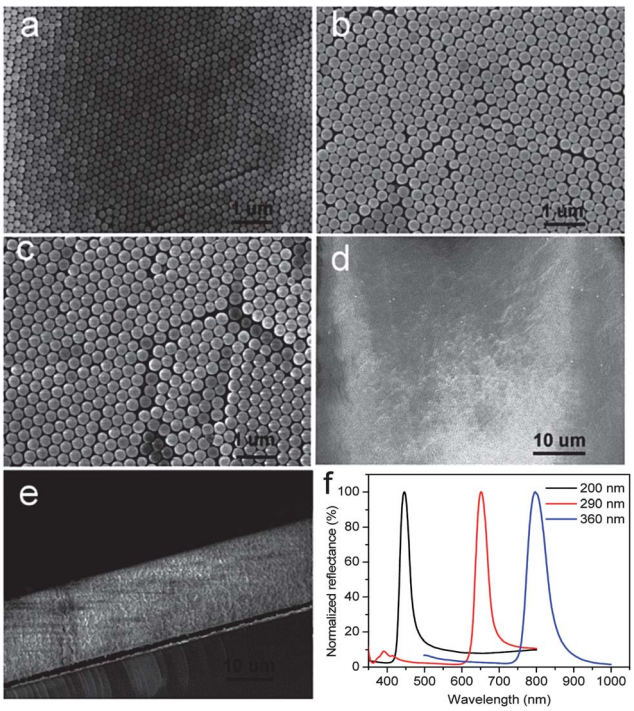

Fig. 2 FESEM top-view images of opal 3D photonic crystals formed from (a) 200 nm, (b and d) 290 nm, (c) 360 nm polystyrene spheres, (e) cross-sectional view of a 290 nm photonic crystal and (f) their normalized reflectance spectra measured at the 20° incidence to the normal.

spontaneous emission rates through the Purcell effect and the effect of inhibited spontaneous emission into undetectable waveguide modes.[24]

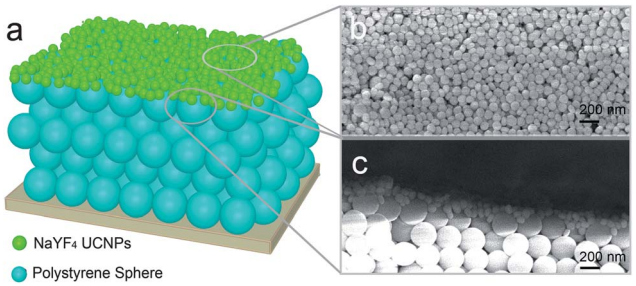

Fig. 3 (a) Schematic illustration of self-assembled photonic crystals with a layer of fluoride UCNPs and the typical FESEM top-view (b) and cross-section (c) images of fluoride UCNPs onto the 3D PC surface.

Another significant attribute to the upconversion emission of nanoparticles is due to the enhanced extraction provided by 3D PCs.[24] To demonstrate the enhanced extraction effect, a series of opal PCs with various transmittance by using different concentrations of 290 nm sized polystyrene spheres were prepared, and their effects on upconversion enhancement were also investigated as the extraction effect only relates to the dispersive properties of the photonic crystal.[24] Fig. 5a shows transmittance spectra of opal PCs prepared with different initial polystyrene sphere concentrations (from 0.1 to 0.5 wt%). The transmittance intensities of those opal PCs reduced monotonously with the increase of polystyrene sphere concentration. The gradually reduced leakage of photons from the rear side of 3D PCs indicates the increased scattering,[20,25] as the polystyrene is transparent in the visible region. The corresponding upconversion intensities of $NaYF_4$:Yb/Er UCNPs increased gradually with the increasing polystyrene sphere concentration (Fig. 5b and c). The trend of upconversion enhancement follows that of the scattering of 3D PCs (Fig. 5). The maximum enhancement factors of about 45 and 38 were achieved for the 540 and 660 nm emission bands of the Er^{3+} ion respectively, on the 3D PC surface prepared with 0.5 wt% polystyrene sphere concentration. These results suggest that the strong scattering and consequent extraction effect largely contributed to the upconversion enhancement of $NaYF_4$:Yb/Er on the 3D PC surface.

To enhance the extraction effect, the reflection peaks of PC surfaces were usually designed to coincide with the emission wavelength of a fluorophore.[18] Nikhil *et al.* reported that the overlap between the emission peak of quantum dots and the reflection peak of the 2-dimensional PC surface would enhance the extraction effect, and 13 times enhancement was observed.[24] In the present cases, although 3D PCs could provide a wide range of wavelengths for resonance with emission peaks of 540 and 660 nm in $NaYF_4$:Yb/Er UCNPs to improve the extraction efficiency (Fig. S3b, ESI†), it is noted that 410 nm emission of the $^2H_{9/2} \rightarrow {}^4I_{15/2}$ transition of $NaYF_4$:Yb/Er, which was not located within the reflection wavelength region of 3D PCs (Fig. S3b†), was also enhanced greatly by 3D PCs with increasing polystyrene sphere concentrations (Fig. S5, ESI†), and 88-fold

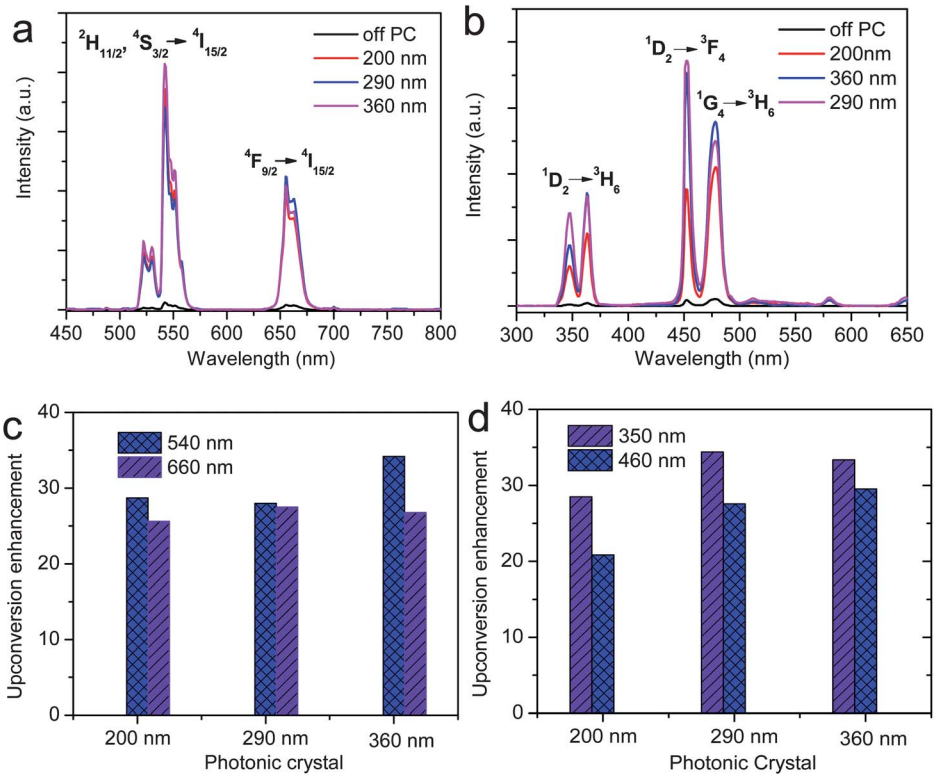

Fig. 4 Upconversion luminescence spectra of $NaYF_4$:Yb/Er (a) and $NaYF_4$:Yb/Tm (b) UCNPs on the surfaces of 3D PCs prepared with different polystyrene sphere sizes at 0.4 wt% concentration, and the corresponding upconversion enhancement factors of characteristic emission bands of 540 nm (510–570 nm) and 660 nm (640–680 nm) in $NaYF_4$:Yb/Er UCNPs (c), and 350 nm (330–380 nm) and 460 nm (440–500 nm) in $NaYF_4$:Yb/Tm UCNPs (d).

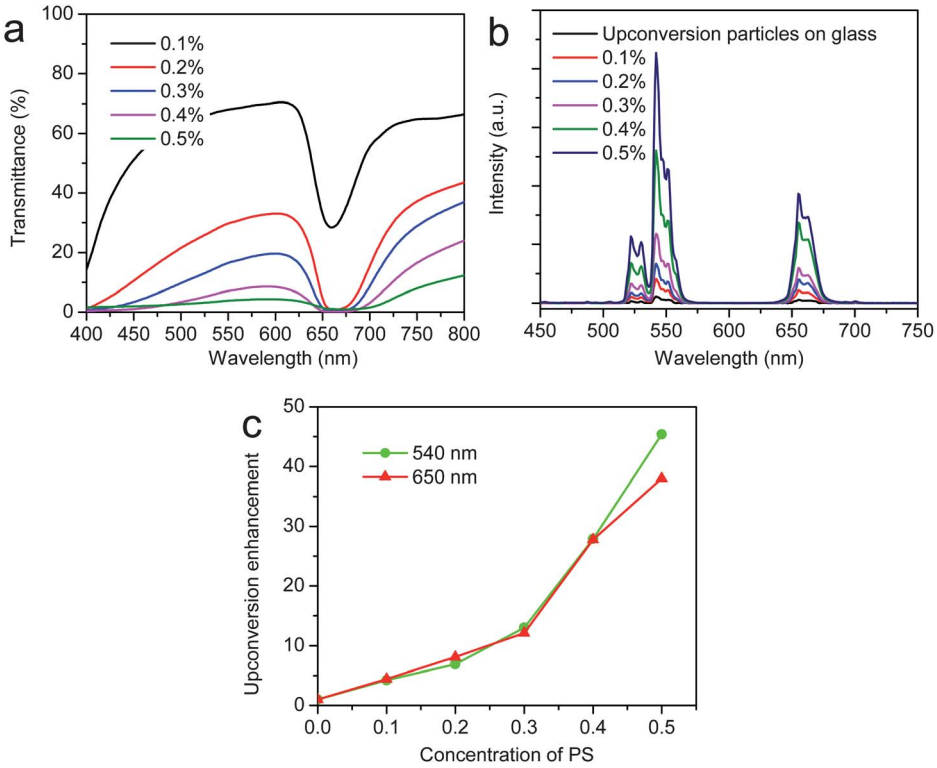

Fig. 5 Transmittance spectra (a) of 3D PCs prepared with different initial concentrations of 290 nm polystyrene spheres, and upconversion spectra (b) and enhancement factors (c) of $NaYF_4$:Yb/Er UCNPs on the surfaces of 3D PCs prepared with different concentrations of 290 nm polystyrene spheres.

upconversion luminescence enhancement was obtained at 0.5 wt% polystyrene sphere concentration. In addition, it is observed that the reflection intensities of the prepared 3D PCs were enhanced slightly with the increase of the concentration of polystyrene spheres from 0.1 to 0.4 wt%, and then diminished when the concentration increased to 0.5 wt% (Fig. S6, ESI†) because of the saturation of the reflectivity of a photonic stop-band,[31] however, upconversion emission intensities of $NaYF_4$:Yb/Er UCNPs increased monotonously with the decreasing transmittance (Fig. 5b and c), and the trend of upconversion enhancement follows that of the scattering of 3D PCs (Fig. 5). It is indicated that the overlap between the emission peak of fluorophores and the reflection peak of the PC surface did not play a significant role in the enhancement of emission intensity through the extraction effect in the present work due to the strong scattering of PCs.

Together, the enhanced absorption in combination with the strong coherent scattering and consequent-extraction effect largely contributed to the upconversion enhancement of nanoparticles on the opal surface. The coincidence of the reflection peak of PCs with the emission wavelength of fluorophores did not play a significant role in the enhancement of extraction effect as the strong scattering of PCs. Due to the similarities of the non-resonant pump excitation field-enhanced absorption (Fig. S2 and Table S1, ESI†) and the strong coherent scattering effects (Fig. S4, ESI†), 3D PCs with different polystyrene sphere sizes enhance the emissions of $NaYF_4$:Yb/Er and $NaYF_4$:Yb/Tm UCNPs in a similar trend and at similar enhancement times (Fig. 4), which further supported the present conclusion. In addition, the enhancement for the short wavelength emission is slightly stronger than that for the long wavelength one in both the Yb/Er and Yb/Tm co-doped samples. This could be due to the lower transmittance in the short wavelength region as shown in Fig. S4.† As lower transmittance indicates higher scattering and stronger consequent extraction effects, the slightly higher enhancement factors for the short wavelength emissions are observed in both the Yb/Er and Yb/Tm co-doped samples.

To demonstrate the use of the UCNPs coupled on the opals in photoelectronic devices, we integrated the 3D PC/$NaYF_4$:Yb/Tm UCNP coupled material with a single-walled CNT-based phototransistor to improve the near-infrared light photoresponsivity. Fig. 6a shows the normalized drain current (I/I_0, where I_0 is the current at $t = 0$) of the photoresponse devices as a function of time for representative four cycles. Here, a source–drain voltage (V_{DS}) of 10 mV was applied in the absence of gate bias. Upon 980 nm near-infrared light irradiation, the drain currents of all the samples increase immediately. Once the incident light was removed, the drain currents dropped back to the ground state. The amperometric curves of the devices shown in Fig. 6a exhibited fast photoresponse and good photostability upon near-infrared light irradiation.[32]

The control experiment with analogous devices prepared with only CNTs shows that the drain current increased by around 0.5% due to the weak absorption of the near-infrared excitation light by CNTs (Fig. 6b).[32] When the carbon nanotubes

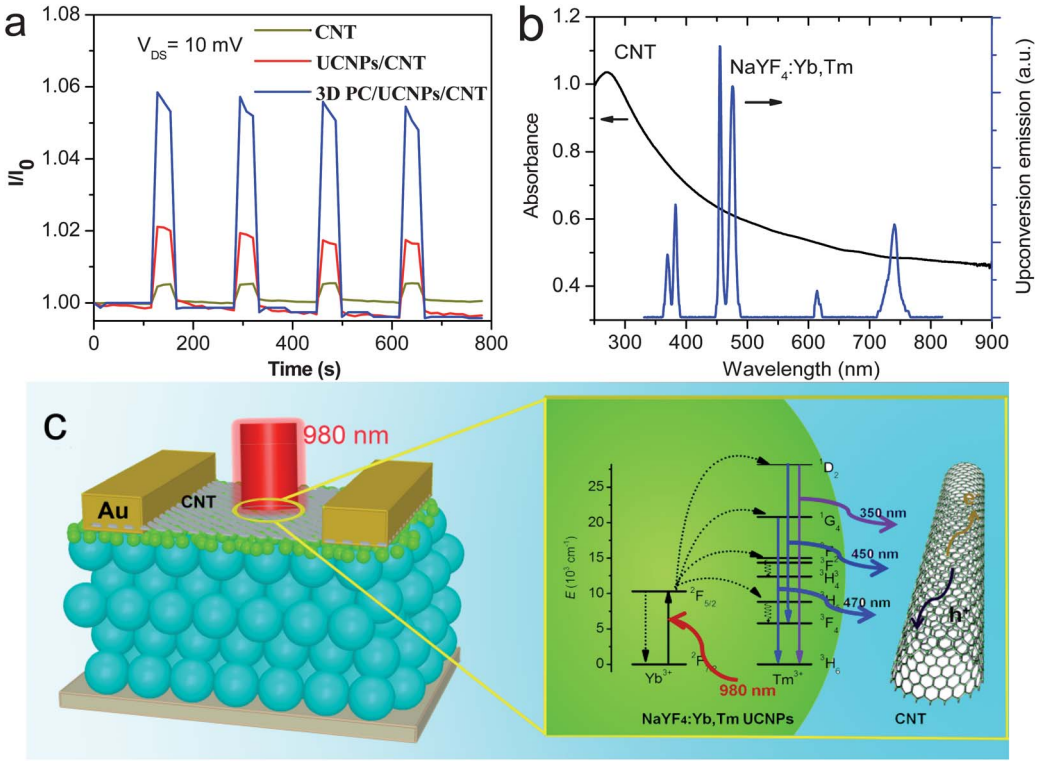

Fig. 6 Real-time measurements of the normalized drain current of the near-infrared photoresponse devices while the 980 nm IR light (200 mW) is switched on and off with V_{DS} 10 mV (a), absorption spectrum of single walled-CNT aqueous solution (b), and the schematic illustration of the enhancement mechanism of near-infrared light photoresponsivity of CNT-based devices by $NaYF_4$:Yb/Tm UCNPs (c). CNT, UCNP/CNT and 3D PC/UCNP/CNT represent the devices prepared with the layers of carbon nanotubes, $NaYF_4$:Yb/Tm UCNP/carbon nanotubes and 3D photonic crystal/$NaYF_4$:Yb/Tm UCNP/carbon nanotubes, respectively.

are coupled with $NaYF_4$:Yb/Tm UCNPs, the photocurrents are enhanced by 3 times in the phototransistor. This indicates that the upconverted photons with higher energy (350 and 450 nm) are readily absorbed by the CNT for charge separation (Fig. 6b and c). The highest photocurrent was found in the device when the $NaYF_4$:Yb/Tm UCNPs coupled on the opal are used for the CNT phototransistor. The current is 10 times higher than that of the device with CNTs only. This clearly shows that the enhanced photoresponsivity of the device is due to the 3D PC surface-enhanced photon upconversion.

Experimental section

Synthesis of Yb/Er and Yb/Tm co-doped $NaYF_4$

Yb/Er and Yb/Tm co-doped $NaYF_4$ UCNPs were synthesized according to the recently reported thermolysis method.[11] For a typical synthesis of $NaYF_4$:Yb/Er, 1.0 mL of YCl_3 (0.78 mol L^{-1}), 1.0 mL of $YbCl_3$ (0.20 mol L^{-1}), 0.5 mL of $ErCl_3$ (0.04 mol L^{-1}), 6 mL of oleic acid and 15 mL of octadecene were added into a 100 mL flask. The solution was heated to 120 °C for 10 min and then to 155 °C for 30 min. After cooling the solution to 60 °C, a solution containing methanol (8 mL), NH_4F (0.148 g) and NaOH (0.1 g) was added into the flask and the solution was maintained at 55 °C for 30 min. Then the resulting solution was heated to 300 °C and maintained for 1.5 h under a nitrogen atmosphere. After heating was stopped, the reaction solution was cooled to room temperature and absolute ethanol was added to precipitate the fluoride UCNPs. The products were isolated by centrifugation.

Self-assembly of opal 3D photonic crystals

The monodisperse carboxylate-modified polystyrene spheres (200, 290 and 360 nm) were diluted with deionized water to form 0.4 wt% suspension and 5 mL of the solution was added into a small vial with the volume of 5 mL. The cleaned glass substrate with 1.0 cm width was fixed in the vial, kept in an oven at 90 °C with the humidity of 90% for 12 h to assemble opals by a vertical deposition method. The prepared UCNPs dispersed in hexane were spin-coated onto the surface of PC slabs.

Fabrication of the device

The single-walled CNT solution (1 mg mL^{-1}) was prepared by adding single-walled CNTs into 1% sodium dodecyl sulphate solution, followed by ultrasonication for 15–20 min. After that, the CNT solution (100 μL) was drop-cast onto the surface of the as-prepared opal 3D PC slab with a layer of $NaYF_4$:Yb/Tm UCNPs (around 1 × 1 cm in size) and dried at 50 °C. Then, gold electrodes (80–100 nm thick) were evaporated on the samples through a metal mask to form a 200 μm gap where light is illuminated.

Characterization

Field-emission scanning electron microscopy micrographs were taken using a JEOL JSM-6340 instrument. XRD patterns were recorded using a Shimadzu thin film diffractometer equipped with a Cu Kα radiation source. The reflectance and transmittance spectra were measured on a spectrophotometer (Varian, Cary 5000). Upconversion spectra and lifetimes were determined at room temperature under excitation of a 980 nm CW diode laser. The power density of the 980 nm laser source was 4 W cm^{-2}. The signal was dispersed using a 750 mm monochromator combined with suitable filters, and detected using a photomultiplier tube (Hamamatsu R928) using a standard lock-in amplifier technique. The chopper wheel was replaced by a homemade one and the repetition rate of the mechanical chopper was maintained at 500 Hz to generate pulses with a pulse width of 0.15 ms. The detector output was stored on a digital phosphor oscilloscope (Tektronix DPO 7254) and averaged over 500 periods to improve the signal-to-noise ratio. Electrical properties were monitored with a Keithley semiconductor parameter analyser, model 4200-SCS.

Conclusions

In conclusion, we have demonstrated a new method to use fluoride UCNPs coupled on opal 3D PCs for improved near-infrared photoresponse. We show that the enhanced emission of more than 30-fold exhibited by upconversion luminescent nanoparticles is due to the enhanced absorption and extraction provided by opal 3D PCs. By integrating this 3D PC/$NaYF_4$:Yb/Tm UCNP coupled material, we successfully achieved 10 times enhancement of the photoresponsivity of the CNT-based phototransistor to near-infrared light. This is the first demonstration of the fluoride UCNP-3D PC coupled materials in enhancing the photoresponsivity of the CNT-based near-infrared photodetector. This proof-of-concept is potentially applicable not only in other types of phototransistors to enhance the near-infrared light responsivity but also in photovoltaics to harvest photons with subband-gap energies.[32] The 3D PC surface enhanced upconversion luminescence is also highly applicable for improving the detection sensitivity of analytes,[18,33] high resolution cell imaging, *etc.*[34]

Notes and references

1 (*a*) L. T. Su, S. K. Karuturi, J. S. Luo, L. J. Liu, X. F. Liu, J. Guo, T. C. Sum, R. R. Deng, H. J. Fan, X. G. Liu and A. I. Y. Tok, *Adv. Mater.*, 2013, **25**, 1603; (*b*) G. B. Shan and G. P. Demopoulos, *Adv. Mater.*, 2010, **22**, 4373; (*c*) S. Sarkar, B. Meesaragandla, C. Hazra and V. Mahalingam, *Adv. Mater.*, 2013, **25**, 856; (*d*) D. Chen, Y. Wang and M. Hong, *Nano Energy*, 2012, **1**, 73.

2 (*a*) F. Wang, Y. Han, C. S. Lim, Y. Lu, J. Wang, J. Xu, H. Chen, C. Zhang, M. Hong and X. Liu, *Nature*, 2010, **463**, 1061; (*b*) E. Downing, L. Hesselink, J. Ralston and R. Macfarlane, *Science*, 1996, **273**, 1185.

3 L. M. Yao, J. Zhou, J. L. Liu, W. Feng and F. Y. Li, *Adv. Funct. Mater.*, 2012, **22**, 2667.

4 F. Zhang, Q. H. Shi, Y. C. Zhang, Y. F. Shi, K. L. Ding, D. Y. Zhao and G. D. Stucky, *Adv. Mater.*, 2011, **23**, 3775.

5 (*a*) T. Rantanen, M. L. Järvenpää, J. Vuojola, K. Kuningas and T. Soukka, *Angew. Chem., Int. Ed.*, 2008, **120**, 3871; (*b*) T. H. Ji, N. Qie, J. M. Wang, Y. Y. Hua and Z. J. Ji, *Spectrosc. Spectral Anal.*, 2013, **33**, 642; (*c*) W. Wei, T. C. He, X. Teng, S. X. Wu, L. Ma, H. Zhang, J. Ma, Y. H. Yang, H. Y. Chen, Y. Han, H. D. Sun and L. Huang, *Small*, 2012, **8**, 2271; (*d*) Q. Q. Su, S. Y. Han, X. J. Xie, H. M. Zhu, H. Y. Chen, C. K. Chen, R. S. Liu, X. Y. Chen, F. Wang and X. G. Liu, *J. Am. Chem. Soc.*, 2012, **134**, 20849; (*e*) J. V. Garcia, J. P. Yang, D. K. Shen, C. Yao, X. M. Li, R. Wang, G. D. Stucky, D. Y. Zhao, P. C. Ford and F. Zhang, *Small*, 2012, **8**, 3800.

6 (*a*) G. Tian, Z. J. Gu, L. J. Zhou, W. Y. Yin, X. X. Liu, L. Yan, S. Jin, W. L. Ren, G. M. Xing, S. J. Li and Y. L. Zhao, *Adv. Mater.*, 2012, **24**, 1226; (*b*) B. Dong, B. S. Cao, Y. Y. He, Z. Liu, Z. P. Li and Z. Q. Feng, *Adv. Mater.*, 2012, **24**, 1987.

7 Y. S. Liu, D. T. Tu, H. M. Zhu, R. F. Li, W. Q. Luo and X. Y. Chen, *Adv. Mater.*, 2010, **22**, 3266.

8 H. Schäfer, P. Ptacek, K. Kömpe and M. Haase, *Chem. Mater.*, 2007, **19**, 1396.

9 (*a*) H. S. Qian, H. C. Guo, P. C. L. Ho, R. Mahendran and Y. Zhang, *Small*, 2009, **5**, 2285; (*b*) D. Chen and Y. Wang, *Nanoscale*, 2013, **5**, 4621.

10 (*a*) F. Wang, R. R. Deng, J. Wang, Q. X. Wang, Y. Han, H. M. Zhu, X. Y. Chen and X. G. Liu, *Nat. Mater.*, 2011, **10**, 968; (*b*) F. Wang and X. Liu, *Chem. Soc. Rev.*, 2009, **38**, 976; (*c*) W. Niu, S. Wu, S. Zhang, J. Li and L. Li, *Dalton Trans.*, 2010, **40**, 3305; (*d*) W. Niu, S. Wu and S. Zhang, *J. Mater. Chem.*, 2011, **20**, 9113.

11 M. Saboktakin, X. C. Ye, S. J. Oh, S. H. Hong, A. T. Fafarman, U. K. Chettiar, N. Engheta, C. B. Murray and C. R. Kagan, *ACS Nano*, 2012, **6**, 8758.

12 S. Schietinger, T. Aichele, H. Q. Wang, T. Nann and O. Benson, *Nano Lett.*, 2010, **10**, 134.

13 P. Y. Yuan, Y. H. Lee, M. K. Gnanasammandhan, Z. P. Guan, Y. Zhang and Q. H. Xu, *Nanoscale*, 2012, **4**, 5132.

14 (*a*) N. Liu, W. P. Qin, G. S. Qin, T. Jiang and D. Zhao, *Chem. Commun.*, 2011, **47**, 7671; (*b*) W. Feng, L. D. Sun and C. H. Yan, *Chem. Commun.*, 2009, 4393; (*c*) F. Zhang, G. B. Braun, Y. F. Shi, Y. C. Zhang, X. H. Sun, N. O. Reich, D. Y. Zhao and G. Stucky, *J. Am. Chem. Soc.*, 2010, **132**, 2850.

15 W. H. Zhang, F. Ding and S. Y. Chou, *Adv. Mater.*, 2012, **24**, Op236.

16 (*a*) L. Sudheendra, V. Ortalan, S. Dey, N. D. Browning and I. M. Kennedy, *Chem. Mater.*, 2011, **23**, 2987; (*b*) H. P. Paudel, L. L. Zhong, K. Bayat, M. F. Baroughi, S. Smith, C. K. Lin, C. Y. Jiang, M. T. Berry and P. S. May, *J. Phys. Chem. C*, 2011, **115**, 19028.

17 A. Pokhriyal, M. Lu, C. S. Huang, S. Schulz and B. T. Cunningham, *Appl. Phys. Lett.*, 2010, **97**, 121108.

18 A. Pokhriyal, M. Lu, V. Chaudhery, C. S. Huang, S. Schulz and B. T. Cunningham, *Opt. Express*, 2010, **18**, 24793.

19 E. Fluck, N. F. van Hulst, W. L. Vos and L. Kuipers, *Phys. Rev. E: Stat., Nonlinear, Soft Matter Phys.*, 2003, **68**, 015601.

20 K. Ishizaki and S. Noda, *Nature*, 2009, **460**, 367.

21 V. Chaudhery, M. Lu, C. S. Huang, S. George and B. T. Cunningham, *J. Fluoresc.*, 2011, **21**, 707.
22 N. Ganesh, P. C. Mathias, W. Zhang and B. T. Cunningham, *J. Appl. Phys.*, 2008, **103**, 094320.
23 K. Bittkau, R. Carius, A. Bielawny and R. B. Wehrspohn, *J. Mater. Sci.: Mater. Electron.*, 2008, **19**, S203.
24 N. Ganesh, W. Zhang, P. C. Mathias, E. Chow, J. A. N. T. Soares, V. Malyarchuk, A. D. Smith and B. T. Cunningham, *Nat. Nanotechnol.*, 2007, **2**, 515.
25 Z. Yin, Y. S. Zhu, W. Xu, J. Wang, S. Xu, B. Dong, L. Xu, S. Zhang and H. W. Song, *Chem. Commun.*, 2013, **49**, 3781.
26 G. Chen, T. Y. Ohulchanskyy, R. Kumar, H. Ugren and P. N. Prasad, *ACS Nano*, 2010, **4**, 3163.
27 (*a*) F. Zhang and D. Zhao, *ACS Nano*, 2008, **3**, 159; (*b*) Z. Li, Y. Zhang and S. Jiang, *Adv. Mater.*, 2008, **20**, 4765.
28 (*a*) C. W. Cheng, S. K. Karuturi, L. J. Liu, J. P. Liu, H. X. Li, L. T. Su, A. I. Y. Tok and H. J. Fan, *Small*, 2012, **8**, 37; (*b*) L. J. Liu, S. K. Karuturi, L. T. Su and A. I. Y. Tok, *Energy Environ. Sci.*, 2011, **4**, 209.
29 (*a*) J. Wang, F. Wang, C. Wang, Z. Liu and X. G. Liu, *Angew. Chem., Int. Ed.*, 2011, **50**, 10369; (*b*) Z. Chen, H. Chen, H. Hu, M. Yu, F. Li, Q. Zhang, Z. Zhou, T. Yi and C. Huang, *J. Am. Chem. Soc.*, 2008, **130**, 3023; (*c*) G. Wang, Q. Peng and Y. Li, *J. Am. Chem. Soc.*, 2009, **131**, 14200; (*d*) C. Yan, A. Dadvand, F. Rosei and D. F. Perepichka, *J. Am. Chem. Soc.*, 2010, **132**, 8868.
30 Q. Zhan, J. Qian, H. Liang, G. Somesfalean, D. Wang, S. He, Z. Zhang and S. Andersson-Engels, *ACS Nano*, 2011, **5**, 3744.
31 Y. Q. Zhang, J. X. Wang, Z. Y. Ji, W. P. Hu, L. Jiang, Y. L. Song and D. B. Zhu, *J. Mater. Chem.*, 2007, **17**, 90.
32 T. Murakami, H. Nakatsuji, M. Inada, Y. Matoba, T. Umeyama, M. Tsujimoto, S. Isoda, M. Hashida and H. Imahori, *J. Am. Chem. Soc.*, 2012, **134**, 17862.
33 M. Z. Li, F. He, Q. Liao, J. Liu, L. Xu, L. Jiang, Y. L. Song, S. Wang and D. B. Zhu, *Angew. Chem., Int. Ed.*, 2008, **47**, 7258.
34 (*a*) F. J. G. de Abajo, *Science*, 2013, **339**, 917; (*b*) F. Bonaccorso, Z. Sun, T. Hasan and A. C. Ferrari, *Nat. Photonics*, 2010, **4**, 611.